

DYNAMIC BEHAVIOR OF VORTEX SHEDDING FROM AN OSCILLATING THREE-DIMENSIONAL AIRFOIL

Hiroaki Hasegawa*, Kennichi Nakagawa**

*Department of Mechanical Engineering, Akita University
1-1 Tegata gakuen-machi Akita-shi, Akita 010-8502, Japan

E-mail: hhasegaw@mech.akita-u.ac.jp,

** Graduate school of Engineering & Resource Science, Akita University
1-1 Tegata gakuen-machi Akita-shi, Akita 010-8502, Japan

E-mail: n-ken@mech.akita-u.ac.jp

Keywords: *Vortex, Unsteady Flow, Pitching Oscillation, Wake*

Abstract

Flow fields around an oscillating airfoil are extremely unsteady because the change direction of leading edge produces unsteady vortex motions. Visualizations of flows relevant to the unsteady propulsive systems of birds, insects, and fishes are rare and inconclusive. To evaluate the force correctly, it is necessary to know the unsteady properties determined from the vortex dynamics. The purpose of this study is to investigate the relationship between unsteady fluid forces and the vortex behaviors of a three-dimensional airfoil during pitch-oscillating motion. The measurements of unsteady fluid force under the pitch-oscillating motion of a discoid airfoil are carried out in a wind tunnel. The flow structures due to the behaviour of vortices in the wake are strongly affected by the reduced frequency, and the fluid force acting on the airfoil model increases with increasing the reduced frequency. Therefore, unsteady fluid force variations are significantly related to the vortex behaviour during the one oscillating cycle because the peak in the unsteady fluid force is observed when the vortex shed from the airfoil edge becomes large in the wake.

1. Introduction

Many researches on the unsteady flow at the low Reynolds number region have been attracted in recent years by an interest in the

micro-air-vehicle. Studies of unsteady propulsion system of birds, insects, and fish are few and inconclusive. The wings of travelling birds and insects execute complex motions whose most obvious component is flapping, whereas for a fishtail the most obvious component is pitching. In recent years, considerable research efforts in a number of institutions have been devoted to advancing understanding of the propulsive mechanism of flapping wings. It has been noted that the unsteady fluid force plays an important role in biological flight. A quasi-steady approach used to predict the fluid force in flapping flight yielded errors in predicting the fluid forces acting on a wing, suggesting that flight is impossible[1,2]. However, because biological flight does occur, the effect of unsteady fluid forces must be important to the flight mechanism. These forces must also be considered when estimating the propulsive force of swimmers doing the front crawl. It has been already known that the propulsive force generated by hand motion is dominant in the front crawl because the propulsive force obtained through hand movements is larger than that generated by foot movements.

The question of whether propulsion in swimming is primarily due to lift or drag appeared to have been settled in the early 1970s. Before then, it was believed that the best way to propel the body forward was to pull the hand directly backward to use drag forces. The first

important contribution related to the mechanism of propulsion in a swimming stroke was made by Counsilman[3]. That mechanism has been examined by dividing the force into two components: a lift component normal to the hand motion and a drag one parallel to it. He pointed out the importance of the lift force relative to that of the drag force. The actual motion of a hand in swimming is obviously unsteady, and the time-dependent fluid forces, called dynamic lift, have to be considered. In fact, when predicting the hand force in swimming, the quasi-steady-state approach, which depends on the assumption that the flow at each instant is nearly steady, has led to errors in predicting the fluid forces acting on a hand under unsteady conditions. Quasi-steady analysis underestimates the fluid forces[4]. These discrepancies arise from the simplistic assumption that the flow has no temporal changes. Unsteady effects occurred by the change action of airfoil, such as the directional changes of angle of attack, must be considered when investigating the basic properties of force. Flow fields around an oscillating airfoil are extremely unsteady because the change direction of leading edge produces unsteady vortex motions. To evaluate the force correctly, it is necessary to know the unsteady properties determined from the vortex dynamics. The aim of this study is to elucidate the propulsive vortical signature of a discoid airfoil in a periodic pitch-oscillating motion, which represents the fundamental unsteady motion. In particular, the flow visualization technique is used to better understand the relationship between the vortical disturbances produced by an oscillating airfoil and the unsteadiness in the oscillation corresponding to the reduced frequency.

In the present study, wind tunnel tests using an airfoil model simulating a hand were carried out to elucidate unsteadiness in propulsion in swimming. In general, there are many parameters to be considered for the unsteady phenomena, and therefore it is difficult to elucidate unsteady mechanisms. Complex parameters affecting unsteady phenomena can easily be changed in a wind tunnel test. To investigate the unsteady fluid forces on a human

hand, the three-dimensional characteristics of the test model must be considered. In order to understand the generating mechanism of unsteady fluid forces, the numerical and experimental approaches have been carried out [5]. However, most of the experimental studies have been performed by using a two-dimensional airfoil[6,7], and therefore for a three-dimensional model the generating mechanism of unsteady fluid forces has not been completely clarified yet.

2. Experimental Apparatus and Methods

2.1 Experimental apparatus

Experiments were performed in a low speed wind tunnel. Figure 1 shows a schematic of the experimental setup and the coordinate system used to describe the flow field. The origins of coordinates X , Y , and Z are defined as the center of the model. The test section inlet dimensions were 300×300 mm, and the freestream turbulence intensity was less than 0.2 percent within the operating range. The test model, a discoid airfoil, has NACA0015 profile, and the schematic of the model is shown in Fig.2. The discoid airfoil has a chord c of 150 mm and a span of 150 mm, and its maximum thickness was 37.5 mm. The airfoil edge was of a smoothed, half-round shape. Pitching motion with a sinusoidal wave was achieved using a five-phase stepping motor with 0.072 deg per 1 step around its mid-chord axis. The measurement error of a model's angle of attack can be evaluated within an error of $\pm 0.5\%$ using a potential meter. The fluid forces acting on the model were measured using a ring structure balance system. The balance could simultaneously detect all of the lift and drag as functions of time during pitch-oscillating motion. The balance system was described in a previous report[8], and hence its details are omitted here.

2.2 Experimental method

The freestream Reynolds number was defined as $Re = cU_0/\nu$, where U_0 is the freestream velocity, and ν is the kinematic

viscosity of air. The experiments described here were performed for $Re = 7.5 \times 10^4$, which corresponds to the Reynolds number range for a swimmer's hand. The pitch-oscillating motion is defined by a sinusoidal wave function, and the angle of attack α of the model varied with the function $\alpha = A\sin(2\pi ft) + \alpha_c$, where A is the amplitude, f is the oscillation frequency, and α_c is the angle of the pitching center. The velocity is denoted by the components (u, v, w) in the directions (X, Y, Z) . The flow field was measured using a particle image velocimetry (PIV) method, the PIV system mainly consists of a Nd-YAG laser (G8000; Katoukouken Co.) and a digital high speed video camera (FASTCAM-1024PCI 100K; Photron Ltd.) in this experiment. The laser light must be intense to adapt PIV technique to a wide region around the airfoil. The laser light sheet illumination of particle-seeded flow allows derivation of the speed and direction of the flow in the plane from the displacements of the particles. The flow field is estimated using the ensemble average velocity during several pitching cycles. Flow visualization was performed using a smoke method. The smoke method was used to observe the behavior of the vortex shedding from the airfoil edge.

To capture the behavior of the vortex, titanium tetrachloride is dropped to the airfoil surface. Titanium tetrachloride is liquid at normal temperature and reacts with present moisture in the airstream to form visible fumes. If a few drops of the liquid are placed on the edge of the airfoil model, dense white smoke is generated in the near-wake recirculating region and the wake flow is made visible. Sheet light illuminates from two sides in the $X-Z$ and $Y-Z$ planes, and time sequential flow patterns produced by the pitching oscillation were captured by a digital high speed video camera. For measurements in the $X-Z$ plane, the horizontal laser sheet is deflected by a mirror set at the top of the test section (see Fig.1). The level position of the laser sheet is adjusted to change the illuminated plane in the spanwise direction with respect to the vortex behavior in the wake of the airfoil at various spanwise positions.

3. Results and Discussion

3.1 Fluid force characteristics for a discoid airfoil

In the present study, during oscillation, the angles of attack of the airfoil always become large due to the large angle of the pitching center ($\alpha_c=90\text{deg}$), and hence the airfoil indicates the stalled state. That is, the unsteady fluid force investigation was performed by the drag force because no significant variations in lift curve were found during the pitch-oscillating motion. Figure 3 shows the drag curves under stationary and dynamic conditions.

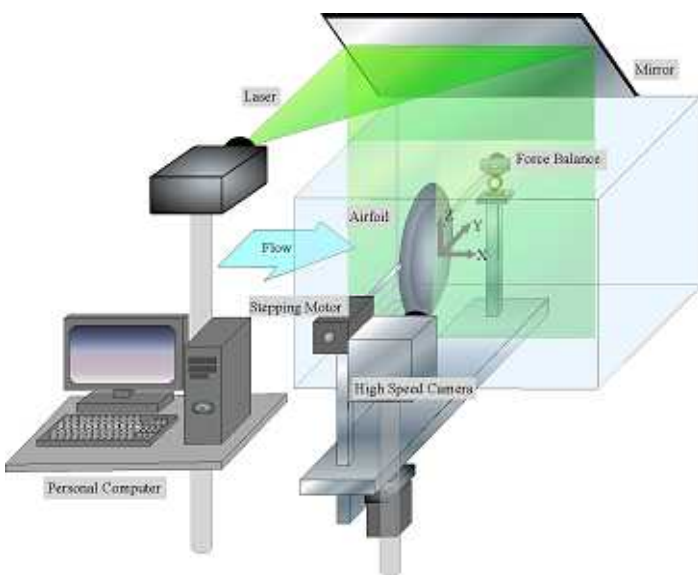


Fig.1 Experimental apparatus and force balance system

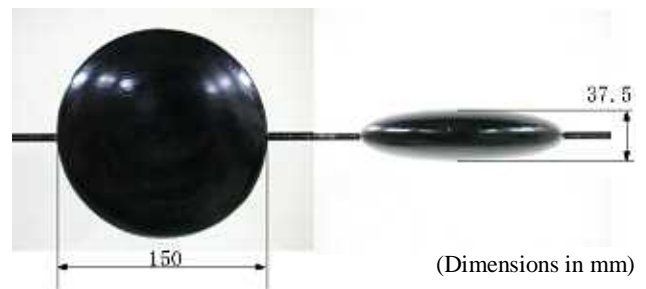


Fig.2 Schematic of discoid airfoil

The static forces are measured at regular intervals of 1.0 deg. Upstroke and downstroke indicated in the figure denote the increment and decrement of the angle of attack, respectively. The drag curve slope is varied at the angle of the pitching center, and the degree of the slope change significantly increases for large reduced frequency. Figure 4 shows drag variations against the non-dimensional time during pitching oscillation. The non-dimensional time t' is defined as $t'=t/T$, where T is total time of one oscillating cycle. The drag coefficient under stationary condition is plotted by considering the airfoil's angle of attack calculated by the non-dimensional time. There are two peaks in the dynamic drag variation during one oscillating cycle, and the variation in drag coefficient becomes more pronounced at high reduced frequency. The ratio of drag under dynamic condition to that under stationary condition for several reduced frequencies is shown in Fig.5. The drag ratio is calculated by averaging the drag value in one pitching cycle. The drag ratio increases with increasing the reduced frequency.

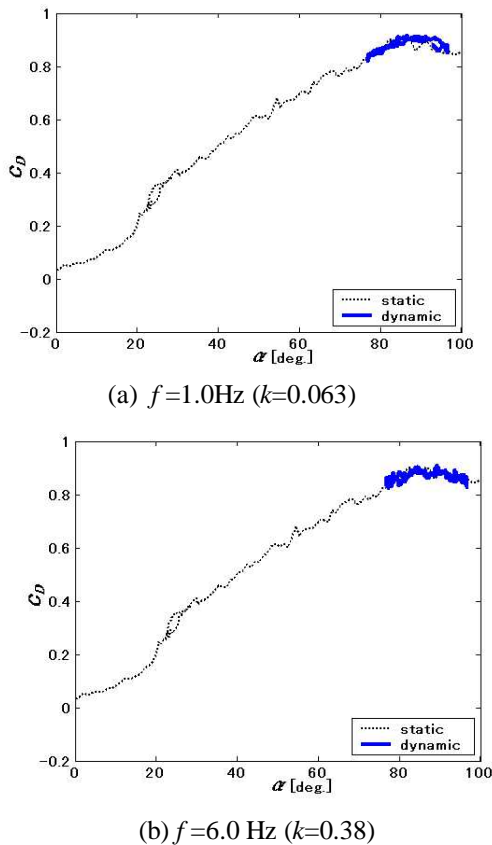


Fig.3 Dynamic drag coefficient curves for $Re=7.5 \times 10^4$ ($A=10$ deg, $\alpha_c=87$ deg).

3.2 Vortex behavior during pitching oscillation

Figure 6 shows the time-sequence of movie frames visualizing vortex generation and development for a pitch-oscillating airfoil in steady flow $U_0=2$ m/s. The present study is focused on the influence of the reduced frequency k ($=\pi fc/U_0$) on the vortex shedding from the airfoil edge and the vortex behavior in the wake. In all cases, the flow begins to separate near the upper edge and the white smoke rolls up in the downstream direction.

For $k=0.2$, the vortex shedding from the edge is convected downstream. The separated vortices are released into the wake and a vortex street is formed. This vortex behavior in the wake is similar to that for $k=0.7$.

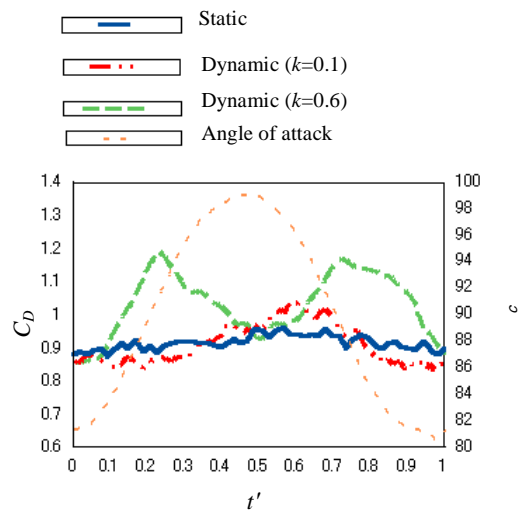


Fig.4 Dynamic drag coefficient curves for $Re=1.0 \times 10^5$ ($A=9$ deg, $\alpha_c=90$ deg).

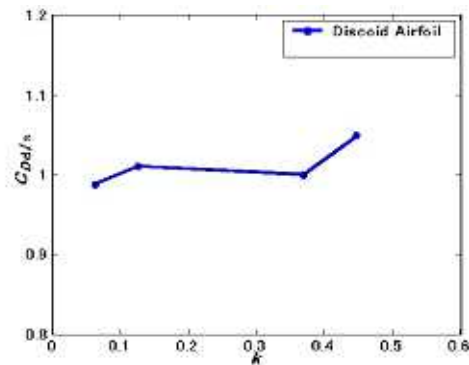


Fig.5 Drag ratio between dynamic and stationary conditions for $Re=7.5 \times 10^4$ ($A=9$ deg, $\alpha_c=90$ deg).

The vortex growth in the wake, marked by the circle in Fig.5 (b), is observed at the instant of changing from downstroke to upstroke ($t'=0.5$).

On the other hand, for $k=2.1$, the separated flow near the airfoil edge rolls up on the leeward surface during downstroke ($t'=0.25$). The vortex grows bigger as non-dimensional time increases. The differences from the case of $k=0.2$ are that 1) the position of the rolled-up vortex is close to the leeward surface and 2) the vortex shedding has already occurred in the downstroke motion. The flow structures due to the behavior of vortices in the wake are strongly affected by the reduced frequency, and the fluid force acting on the airfoil model increases with increasing the reduced frequency, which is mentioned earlier. The non-dimensional time at which the vortex growth is observed coincides with time obtained the peak value in dynamic drag curve ($t'=0.75$).

Therefore, unsteady fluid force variations are significantly related to the vortex behaviour during the one oscillating cycle because the peak in the unsteady fluid force is observed when the vortex shed from the airfoil edge becomes large in the wake at the beginning of the downstroke motion.

3.3 Flow fields around the airfoil

Figure 7 shows contour maps of the vorticity and velocity vectors in the wake of the airfoil. The color bar in the figure indicates the strength of the vorticity. The vortical field in the wake was measured by a PIV method. The vortex which exists near the airfoil edge retains its strength with decreasing angle of attack. In particular, for $k=2.1$, the strong vortex appears near the airfoil edge during downstroke.

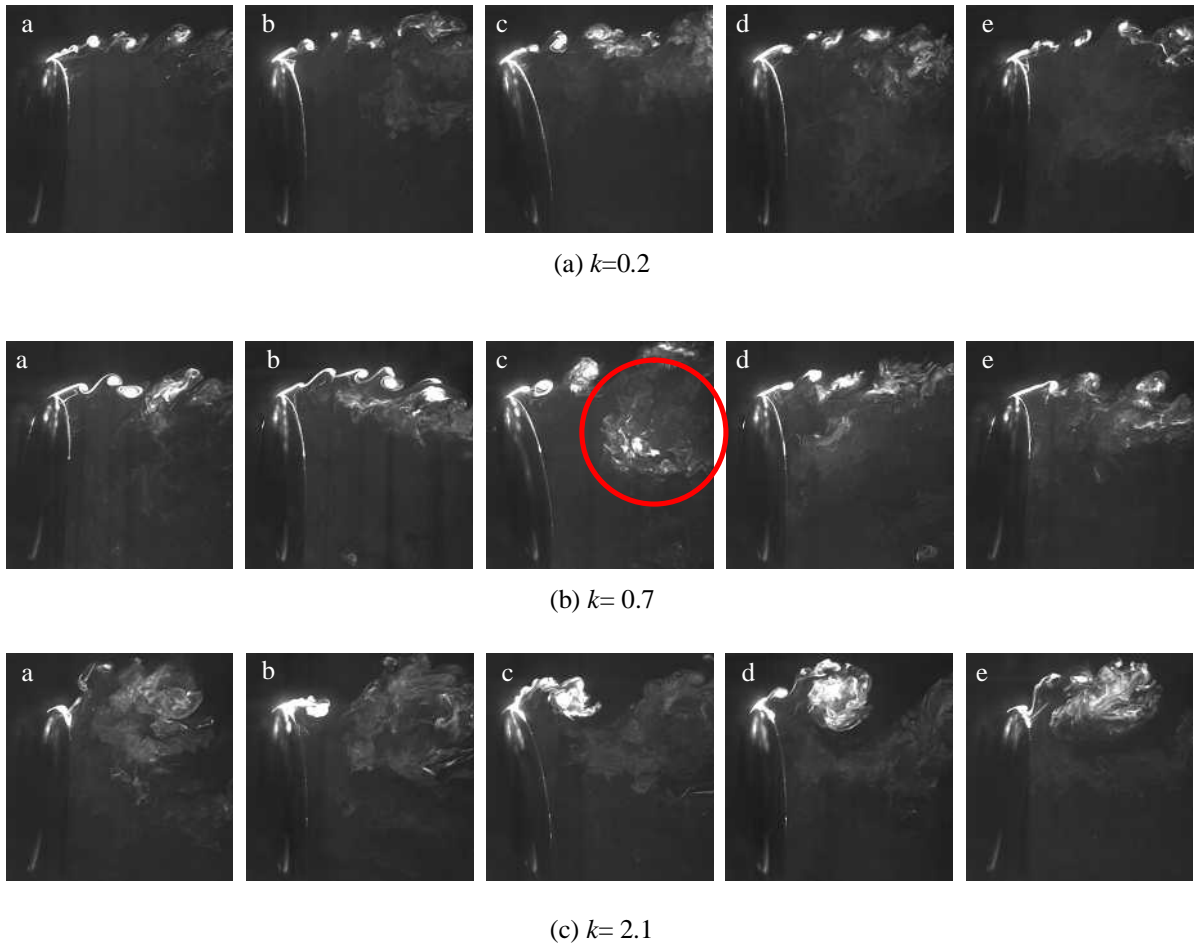


Fig.6 Successive flow patterns during pitch-oscillating motion ($Re=0.2 \times 10^5$, $c=90^\circ$, $y/c=0.0$): (a) $t=0.0$; (b) $t=0.25$; (c) $t=0.50$; (d) $t=0.75$; (e) $t=1.0$

During downstroke of pitch-oscillating motion, the vortex growth promotes due to the pressure difference between the front side (windward side) and back side (lee side) of the airfoil.

The strength of the vortex increases with increasing the reduced frequency, because the vortex growth is significantly related to the relative velocity between the velocities of the airfoil edge and a freestream. That is, the vortex generation and vortex growth around the airfoil occur during downstroke of pitching oscillation because the relative velocity between the velocities of the freestream and the model movement is strongly produced. After that time, during upstroke, the vortex shedding from the airfoil edge occurs.

The fluid forces are effectively produced by the vortices existed around the airfoil and decrease just after the vortices shed from the airfoil edge. The vortex generation and the vortex growth are strongly affected by the reduced frequency, and the peak value of the fluid force variation during pitch-oscillating motion is significantly increased due to the strong vortex generated by high reduced frequency.

4 CONCLUSIONS

In the present study, unsteady fluid forces acting on a discoid airfoil, and vortex behavior into the wake while sinusoidal pitch- oscillating motion were measured to investigate the relationship between the unsteady fluid force and the vortex behavior. The results are summarized as follows:

- (1) There are two peaks in the fluid force variation during one pitch-oscillating cycle, and the peak value of the fluid force increases with increasing the reduced frequency.
- (2) For $k=0.2$, the vortex shedding from the edge is convected downstream. The separated vortices are released into the wake and a vortex street is formed.
- (3) On the other hand, for $k=2.1$, the separated flow near the airfoil edge rolls up on the leeward surface during the downstroke.
- (4) For $k=2.1$, the position of the rolled-up vortex is close to the leeward surface and the vortex shedding has already occurred in the downstroke motion, in contrast to the case of $k=0.2$.
- (5) During downstroke of pitch-oscillating motion, the vortex growth promotes due to the pressure difference between the front side and back side of the airfoil. The strength of the vortex increases with increasing the reduced frequency.

References

- [1] S. P. Sane. The aerodynamics of insect flight, *Journal of Experimental Biology* 206, 4191-4208, 2003.
- [2] C. P. Ellington, C. van den, Berg, A. P. Willmott and A. L. R. Thomas. Leading-edge vortices in insect flight. *Nature* 384, pp.626-630, 1996.
- [3] J. E. Counsilman. The application of Bernoulli's principle to human propulsion in water. *Prop. ternational Symposium on Biomechanics of Swimming, Water Polo and Diving*, where it took place pp. 59-71,1970.
- [4] M. A. M. Berger, A. P. Hollander and G. De Groot. Determining propulsive force in front crawl swimming: A comparison of two methods, *J. Sport Sciences*, 17, pp. 97-105, 1999.

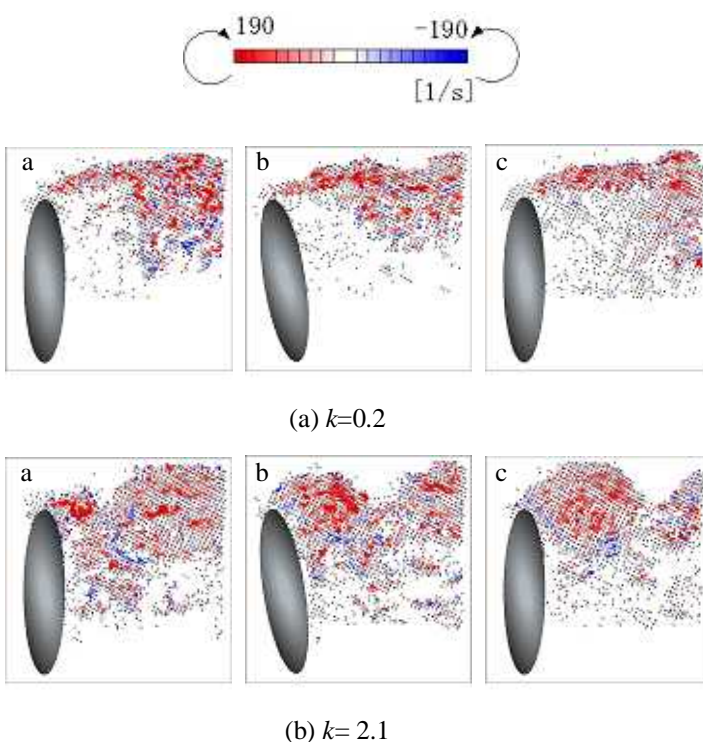


Fig.7 Flow fields in the wake of a discoid airfoil during pitch-oscillating motion ($Re=0.2 \times 10^5$, $\alpha_c=90^\circ$, $y/c=0.0$):

(a) $t = 0.25$; (b) $t = 0.50$; (c) $t = 0.75$

- [5] H. Oshima and B. R. Ramaprian. Velocity measurements over a pitching airfoil. *AIAA JOURNAL*, Vol. 35, No. 1, 119-126, 1997.
- [6] P.Ghosh Choudhuri and D.D. Knight. Two-dimensional unsteady leading-edge separation on a pitching airfoil. *AIAA JOURNAL*, Vol. 32, No.4, pp.673-681, 1994.
- [7] Y.W. Jung, S.O. Park. Vortex-shedding characteristics in the wake of an oscillating airfoil at low Reynolds number. *JOURNAL OF FLUIDS AND STRUCTURES*, 20, pp.451-464, 2005.
- [8] H. Hasegawa, A. Nakamura and K. Tanaka, Unsteady fluid forces and vortical structure acting on a three-dimensional airfoil. *Proc. 12th Asian Congress of Fluid Mechanics*, 12ACFM-T-2C-2, 2008.

Copyright Statement

The authors confirm that they, and/or their company or organization, hold copyright on all of the original material included in this paper. The authors also confirm that they have obtained permission, from the copyright holder of any third party material included in this paper, to publish it as part of their paper. The authors confirm that they give permission, or have obtained permission from the copyright holder of this paper, for the publication and distribution of this paper as part of the ICAS2010 proceedings or as individual off-prints from the proceedings.